NIH-PA Author Manuscript

Molecular Imaging: Current Status and Emerging Strategies

Marybeth A. Pysz, Ph.D.[1], **Sanjiv S. Gambhir, M.D., Ph.D.**[1,2], and **Jürgen K. Willmann, M.D.**[1,*]

[1]Department of Radiology, Molecular Imaging Program at Stanford, Stanford University School of Medicine, Stanford, CA, USA

[2]Department of Bioengineering, Stanford University, Stanford, CA, USA

Abstract

In vivo molecular imaging has a great potential to impact medicine by detecting diseases in early stages (screening), identifying extent of disease, selecting disease- and patient-specific therapeutic treatment (personalized medicine), applying a directed or targeted therapy, and measuring molecular-specific effects of treatment. Current clinical molecular imaging approaches primarily use PET- or SPECT-based techniques. In ongoing preclinical research novel molecular targets of different diseases are identified and, sophisticated and multifunctional contrast agents for imaging these molecular targets are developed along with new technologies and instrumentation for multimodality molecular imaging. Contrast-enhanced molecular ultrasound with molecularly-targeted contrast microbubbles is explored as a clinically translatable molecular imaging strategy for screening, diagnosing, and monitoring diseases at the molecular level. Optical imaging with fluorescent molecular probes and ultrasound imaging with molecularly-targeted microbubbles are attractive strategies since they provide real-time imaging, are relatively inexpensive, produce images with high spatial resolution, and do not involve exposure to ionizing irradiation. Raman spectroscopy/microscopy has emerged as a molecular optical imaging strategy for ultrasensitive detection of multiple biomolecules/biochemicals with both *in vivo* and *ex vivo* versatility. Photoacoustic imaging is a hybrid of optical and ultrasound modalities involving optically-excitable molecularly-targeted contrast agents and quantitative detection of resulting oscillatory contrast agent movement with ultrasound. Current preclinical findings and advances in instrumentation such as endoscopes and microcatheters suggest that these molecular imaging modalities have numerous clinical applications and will be translated into clinical use in the near future.

INTRODUCTION

Molecular imaging is defined as the ability to visualize and quantitatively measure the function of biological and cellular processes *in vivo*.[1, 2] While anatomical imaging plays a major role in medical imaging for diagnosis, surgical guidance/followup, and treatment monitoring, the rapidly evolving field of molecular imaging promises improvements in specificity and quantitation for screening and early diagnosis, focused and personalized therapy, and earlier treatment follow-up. The main advantage of *in vivo* molecular imaging is its ability to characterize pathologies of diseased tissues without invasive biopsies or surgical procedures, and with this information in hand, a more personalized treatment planning regimen can be applied. For example, recent strategies for treatment of breast cancer involve combinations of several chemotherapeutic drugs that target epidermal growth

Corresponding Author: Jürgen K. Willmann, M.D., Department of Radiology, Stanford University School of Medicine, 300 Pasteur Drive, Room H1307, P: 650-723-5424, Fax: 650-723-1909, willmann@stanford.edu.

factor receptor types I and 2 (EGFR and HER2/neu), mammalian target of rapamycin (mTor), estrogen receptor, and/or histone deacetylase, among others; however, the most effective strategy is dependent on the molecular profile of the tumor (e.g., HER2/neu-targeted therapy is only effective in HER2-positive breast cancers).[3] *In vivo* molecular imaging can be used to identify and quantify the molecular marker profile (e.g., EGFR, HER2) of the tumor without the invasiveness of a surgical biopsy and time associated with pathological characterization. The personalized medicine approach is especially important for determining the best care for patients with advanced stage cancers and poor prognosis - in this case, the risk of exposure to unwanted side-effects of therapy may outweigh the quality of remaining life.

Recent preclinical advances in molecular imaging contrast agents have demonstrated the ability to multiplex nano- and/or microparticles with several entities (Figure 1): 1) a molecule for targeting to a specific tissue/disease marker (binding ligand); 2) a molecule that allows detection of the agent with different imaging modalities; and, 3) a direct attachment or system (e.g., Doxel is a liposome encapsulation of doxirubicin, a cytotoxic drug which inhibits DNA replication), for targeted delivery of a therapeutic drug at the site of interest. For example, Blanco *et al.*[4] describe the direct attachment of the chemotherapy drug, Doxirubicin, to a superparamagnetic iron oxide (SPIO) nanoparticle, which is then encapsulated in liposomes coated with RGD-peptides; thus, these particles specifically attach to tumor angiogenic vessels expressing high levels of $\alpha_V\beta_3$-integrins (protein receptors which bind RGD peptides), and the localization of these magnetic particles can be visualized using magnetic resonance imaging (MRI).

In addition, molecular imaging can be used to measure the response to therapy. Current practices in measuring tumor response to chemotherapy are governed primarily by the Response Evaluation Criteria in Solid Tumors (RECIST) approach, which uses anatomical imaging methods such as computed tomography (CT) or magnetic resonance imaging (MRI) to measure changes in tumor size; however, measurable effects of therapy on tumor volume may take considerable time (weeks to months), indicating that tumor volumetric changes are not an accurate reflection of therapeutic efficacy for some therapies.[5] Molecular imaging has the potential to improve therapeutic monitoring by for example measuring the direct effect of a drug at an earlier time point before overt morphological-anatomical changes become visible on imaging. Most chemotherapeutic/anti-cancer drugs are either directed at specific molecular targets such as epidermal growth factor receptor (EGFR; drugs include erlotinib, cetuximab, and gefitnib), VEGFR (drugs include bevacizumab, sunitinib, axitinib, and vatalanib), estrogen receptor (such as tamoxifen), and EGFR type 2 (also known as ErbB2 or HER2/neu; drug such as trastuzamab), or, they are cytotoxic (drugs include paclitaxel/taxol, fluoruracil, or gemcitabine, among others) to promote tumor cell death. Molecular imaging agents have been designed and tested preclinically in rodent models to image all of the aforementioned molecular targets as well as cellular events such as metabolic activity or apoptosis [6] and, therefore, may be used in the future to monitor treatment effect at the molecular level at earlier time points after treatment initiation than with current imaging strategies.

This article reviews current clinical practices of molecular imaging and highlights promising strategies using optical and acoustic techniques that may be translated into clinical applications in the near future.

Current Clinical Molecular Imaging Strategies

Various imaging modalities are used for medical imaging, including positron emission tomography (PET), single photon emission computed tomography (SPECT), magnetic resonance imaging (MRI), magnetic resonance spectroscopy (MRS), ultrasound (US), and

computed tomography (CT) (Table 1). The majority of molecular imaging in the clinic is currently performed only with PET, SPECT, and MRS imaging. Several PET (Table 2) and SPECT (Table 3) radiotracers are used for medical imaging applications, including oncology, cardiology, and neurology, and are discussed in detail elsewhere (YY et al. and ZZ et al. for PET; AA et al. for SPECT in this issue). MRS is a technique of MRI that measures changes in proton/nuclei excitation/relaxation associated with various metabolites, such as choline, pyruvate, lactate, lipids, and polyamines, among others.[7, 8] Several MRS techniques, including ^{1}H, ^{19}F, ^{31}P, and ^{13}C MRS, have been developed and are reviewed elsewhere (see BB et al. in this issue, and reviews[9, 10]). Clinical applications of MRS include oncology,[9] neurology,[8] and musculoskeletal diseases,[11] among others (Table 4).

Current clinical applications of real-time *in vivo* optical imaging techniques are limited to surface (e.g., skin[12, 13]) or ocular[14, 15] imaging since they suffer from limited depth penetration through human tissue (Tables 1 and 4). However, increasing technological advances in endoscopic (e.g., monitoring Barrett's esophagus) and catheter devices (e.g., imaging of atherosclerosis or bladder cancer) for optical coherence tomography(OCT)[15, 16] as well as microscopy hold promise for novel clinical applications (e.g., Wang et al. [17] used a confocal microendoscope with topically-administered fluorescein to image abnormal lesions and colonic pathology THIS IS NOT A CLINICAL TERM – PLEASE WRITE WHAT COLONIC PATHOLGOIES THEY WERE ADDRESSING in patients undergoing colonoscopy). Furthermore, a multi-photon NIRF source, where two or more photons are used to excite the fluorescent dye/nanoparticle, has been integrated in a tomographical scanner and microendoscope; this approach has been used for clinical optical imaging of skin cancer and other dermatological pathologies.[18]

Most of these devices operate by applying photons for excitation, and measuring reflected light. Alternatively, detection can occur by measuring light scattering effects, as in change of energy before and after the photon collides with a molecule – known commonly as the Raman effect[19] (described in detail below). Since the change in energy is dependent upon the strength of the molecular bond which is colliding with the photon, the Raman signal is a series of peaks representing a specific molecular bond.[19, 20] Thus, Raman spectrophotometry is an emerging molecular imaging technique that can acquire multiple molecular signatures with a single image. Raman spectroscopy and other optical imaging techniques have been used in a few clinical applications; however, they are limited in number since fluorescent-based and Raman-spectra contrast agents, including near-infrared fluorescent (NIRF) (advantageous for deeper penetration and low background fluorescence[12]) dyes, quantum dots (NIRF nanoparticles that are very bright and have long life-span[12]), and nanoparticles with surface enhanced Raman scattering (SERS) properties,[20] have not yet been fully evaluated for human use. So far, Raman spectroscopy for analysis of different molecular signatures has been used in the clinic for identifying atherosclerosis [21] as well as for cancer imaging (e.g., breast,[22] colon[23]). Clinical applications of optical imaging are summarized in Table 4 and include: 1) monitoring atherosclerosis-associated inflammation with protease-activated fluorescent probes (representing capthesin-B and matrix metalloprotease (MMP)-2/9 expression);[24] and, 2) imaging of porphyrin (fluoresces blue light) accumulation in highly-proliferating cancer cells. Therefore, agents that can be chemically converted to porphyrin in cells can be added to "highlight" neoplastic cells. For preclinical applications, optical imaging is frequently used for assessment of many molecular contrast agents, drug testing, and for better understanding basic biological processes. However, clinical translation of the large array of preclinical optical molecular imaging strategies (discussed below) will require significant improvements in instrumentation, contrast agent evaluation, and data analysis for molecular quantification. Contrast-enhanced molecular ultrasound is a very attractive molecular imaging strategy since ultrasound imaging 1) is already a clinical imaging modality; 2) is relatively

inexpensive and portable; 3) offers real-time, high resolution imaging; 4) can separate contrast and morphological imaging (with use of harmonics); and, 5) does not involve ionizing irradiation (Table 1). Contrast agents for current use with ultrasound are microspheres – gas-filled (e.g., perfluorobutane), lipid-shelled bubbles that are 1–4 μm in diameter (see Deshpande et al. in this issue). Microbubbles have been used for imaging primarily the micro- and macrovasculature,[25] since their micron size limits them to vascular compartments. Several commercially available microbubbles include: Luminity®/Definity® (Bristol Myers Squibb), Optison™ (GE Healthcare), Sonovue® (Bracco), and Sonozoid™ (Amersham Health).[26] A common clinical application of contrast-enhanced ultrasound imaging with microbubbles involve characterization of focal lesions (e.g. in the liver) based on vascular enhancement patterns using non-targeted microbubbles.[27, 28] Currently, contrast-enhanced ultrasound is not yet advanced to imaging molecular markers in the clinical realm, although ongoing research is directed towards clinical translation of molecularly targeted ultrasound imaging.[29, 30]

In summary, current clinical molecular imaging is mostly performed with PET and SPECT, and several targeted radiopharmaceuticals for both imaging and dual-imaging/therapy are available. Optical, ultrasound, and other hybrid acoustic imaging strategies (e.g., photoacoustic imaging) offer real-time and inexpensive approaches, which may be well suited for routine clinical applications such as early disease detection and screening protocols involving frequent imaging. The following section reviews emerging preclinical developments in optical, ultrasound, and hybrid acoustic imaging.

PRECLINICAL DEVELOPMENTS IN MOLECULAR IMAGING AND POTENTIAL CLINICAL APPLICATIONS

Preclinical molecular imaging in small animals is an invaluable part of evaluating new molecular targets and contrast agents, as well as developing drugs prior to clinical translation.[31, 32] Figure 2 shows the time intensive and expensive preclinical steps involved in molecular target identification, validation, chemical synthesis, and characterization (*in vitro* and *in vivo* testing for activity, specificity, biodistribution, pharmacokinetics, off-target effects, toxicity, etc) for new molecular imaging agents. In fact, the majority of current molecular imaging agents used in the clinic were discovered through these exhaustive preclinical experiments at academic institutions.[32] It is estimated that a molecular imaging agent costs about $150 million over 10 years to create, test, and move to the clinic, ending with a $200–400 million per year revenue for successful contrast agents.[32] The first step(s) for identifying a molecular target begins with understanding and characterizing the biology to find the differences between a healthy and diseased state. For example, since there is an intricate relationship between inflammation and cancer (i.e., chronic inflammation can often promote cancer and cancer onset can promote an inflammatory response), the differences between inflamed and cancer states must be characterized. In general, much focus is directed towards cancer imaging, and several preclinical studies have identified new molecular targets for imaging cancer (Table 5). In addition to imaging the cancer phenotype such as increases in metabolism, proliferation, angiogenesis, hypoxia, and apoptosis, agents have been developed to target specific protein markers expressed on cancer cells or cancer-associated cells (e.g., tumor angiogenic vessels, stroma). These include tumor cell receptors (EGFR, HER2/neu, ER, folate receptor, somatostatin receptor, VEGFR2, urokinase-plasminogen activator (uPA)/receptor (uPAR), among others), integrins, proteases, and prostate-specific membrane antigen (PSMA) (Table 5 and see BB et al. in this issue), among others. Notably, many chemotherapeutic drugs also target these markers, and have been radiolabelled for assessment of biodistribution and pharmacokinetics using non-invasive molecular imaging (Table 5).[31] Continuing preclinical research has not only exploded in molecular target discovery and imaging probe developments, but also in new strategies for

imaging methodologies, especially in the areas of optical and acoustic imaging. With the advent of new, smaller instruments/devices for insertion into the body, molecular imaging strategies with optical and acoustic devices and specific molecular-targeted contrast agents have great potential for translation into the clinic (Figure 3), which is reviewed in the following sections.

Optical Molecular Imaging

A plethora of optical-based molecular imaging techniques are used in preclinical research for evaluating molecular targets of contrast agents (Table 5) and/or of therapeutics as well as characterizing and understanding biology.[16] Although optical imaging currently is not used in many clinical applications, there are several emerging technologies that foster clinical translation.[15] In terms of novel contrast agent development for optical imaging, Weissleder and colleagues pioneered NIRF-protease-activatible probes for imaging cancer and inflammation (e.g., in colon[33, 34] and lung cancer,[35] as well as in atherosclerosis[36]). These "smart" probes involve a dye-quencher system where the fluorescent dye is connected to a quenching molecule by a short linker peptide. When proteases cleave the peptide, the dye and quencher molecules separate by a distance > 100 Å, and the dye transfers energy to the quencher resulting in a release of light.[37] The "smart" probe strategy has great potential for clinical translation since light is only released when the probe has reached its target and is activated; thus, high signal-to-noise ratios can be obtained due to low background signal and minimal non-specific enzymatic cleavage, which is of paramount importance for imaging weak optical imaging signals in the human body.[38] On the microscale device end, optical imaging is progressing towards integrating confocal microscopy with endoscopes and catheters for real-time "biopsies".[16] Contag and colleagues have developed techniques for early detection of colon cancer using a confocal endomicroscope and a fluorescein-conjugated heptapeptide (VRPMPLQ), which bound to dysplastic colonocytes with high affinity, resulting in a sensitivity of 81% and specificity of 82% for detection of colonic neoplasia in patients undergoing colonoscopy.[39] These confocal microscopy techniques with cancer-specific optical probes can be used for *in vivo* early detection of various cancers in the clinic, including, skin, colon, bladder, prostate, and esophageal cancer, among others.[16] Real-time confocal microscopes can also assist in *ex vivo* analyses of tissue biopsies, such as instantaneous quantification of HER2/neu expression in human breast tumors with 3D microscopy and fluorophore-conjugated anti-HER2/neu antibodies.[40]

Another area of optical imaging that is emerging as a promising tool for clinical optical imaging is Raman spectroscopy/microscopy, which measures inelastic light scattering effects to determine molecular signatures.[20] Optical energy in the form of lasers (typically near-infrared range for increased penetration depth) is applied in pulses resulting in an excitation of molecules to an elevated energy level (laser "on" – absorbing a photon) and a relaxation to a new energy level (laser "off" – releasing a photon); this shift in energy is related to the vibrational energy of a molecular bond, and "fingerprints" of molecules can be created by measuring Raman shifts.[19] The vibrational component is a measure of the changing shape of the electron cloud during the shift ("on"/"off" or molecule excitement/ relaxation). For an example of molecular Raman imaging, the specific Raman shift or "fingerprint" of carbon nanotubes is known as G-band ($\sim$1593 cm^{-1}), and carbon nanotubes conjugated to RGD peptides have been used for *in vivo* molecular Raman spectrographic imaging of human glioma tumor xenografts in mice.[41] The most commonly used methods of Raman spectroscopy/microscopy are Surface-enhanced Raman Scattering (SERS) and Coherence Anti-Stokes Raman Scattering (CARS); both SERS and CARS involve methods to obtain a higher Raman signal. [20, 42] The SERS technique involves adding metal nanoparticles (e.g., gold[43]), which absorb the optical energy and create an enhanced Raman signal whereby the metal surface can transfer energy to nearby molecules, and also exhibit

an excited energy (due to metal surface ions absorbing and releasing photons). Like carbon nanotubes, SERS nanoparticles have unique Raman "fingerprints"; however, the Raman signal enhancement due to the localized interactions with the metal surface of the nanoparticle enable picomolar sensitivity, which is ideal for *in vivo* imaging applications. Furthermore, labeling several different SERS nanoparticles with molecular ligands (Figure 1) can provide a measurement of multiple molecules with a single Raman image.[43] CARS is a nonlinear method which involves applying two or more photons to 1) excite the molecule from the ground state to an excited state (higher energy level), and then 2) the second photon can excite the molecule from its relaxed state (i.e., energy level after releasing photon during "off" pulse after first photon absorption) to a new higher energy level; this second tier of vibrational energy is typically ~5 times stronger than Raman signal after only one photon pulse. The CARS technique is often used for high resolution, 3-dimensional microscopy; the advantages are that there is no need for fluorescent markers to label molecules and images can be acquired relatively quickly.[44] Several preclinical studies (Table 5) have utilized SERS (Figure 4) or CARS techniques for *in vivo* molecular imaging of cell receptors (e.g., RGD-carbon nanotubes that bind to $\alpha_V\beta_3$ integrin-expressing tumors/tumor microvessels[45]), enzyme activity,[46] changes in pH,[20, 47] lipid composition,[48] and myelin composition.[49]

Acoustic Molecular Imaging

While contrast-enhanced ultrasound is gaining popularity and support for a variety of clinical applications in both cardiology and radiology [28, 50–55] (Table 1), preclinical research is focused on improving this technology to a molecular-based approach. Microbubbles can be molecularly targeted to disease-specific markers expressed on tissue vasculature (Deshpande et al. in this issue and [56]), such as microvessels in tumors or inflamed tissues. Most preclinical molecular ultrasound imaging studies utilize microbubbles that have a streptavidin, avidin, or biotin moiety incorporated into the lipid shell via a polyethylene glycol (PEG) arm for conjugation of an antibody via a strept(avidin)-biotin chemistry (Figure 5). However, strept(avidin) is immunogenic, and therefore, these microbubbles cannot be used in humans.[50, 57] Nonetheless, the wide availability of antibodies and ease of conjugation to microbubbles provide a basis for proof-of-principle pre-clinical studies. Several studies have utilized antibody- or peptide-biotin-strept(avidin)-conjugated microbubbles to image tumor angiogenic markers, including VEGFR2,[58–64] integrins,[59, 65], and endoglin[61] (see Deshpande et al. article in this issue; Table 5). Other studies have used molecular-targeted microbubbles to image molecular adhesion molecules overexpressed in microvessels of inflamed tissues; these include mucosal addressin cellular adhesion molecule (MadCAM1),[66] vascular cellular adhesion molecule (VCAM1),[54, 67] intracellular adhesion molecule (ICAM1)[68–70] and P-selectin[71–73] (also see Deshpande et al. in this issue). Clinical translation of molecular ultrasound imaging with microbubbles requires several important steps, including development of molecular-targeted microbubbles without the toxic strept(avidin)-biotin chemistry, implementation of quantitative software on clinical ultrasound machines, and a standardized technique for quantification of attached microbubbles (Figure 5). A novel microbubble targeted to kinase insert domain receptor (KDR), the human analog of VEGFR2, was recently developed by fusing a heteropeptide (found to bind KDR with high affinity) to a hydrophilic spacer and lipid to form a heterolipopeptide for attachment to the PEG arm of the microbubble shell (Figure 5).[29, 30] Preclinical evaluation of this KDR-targeted microbubble demonstrated cross-reactivity with mouse VEGFR2, and the ability to monitor anti-angiogenic therapy in human colon tumor-bearing mice,[30] providing the groundwork for a translation of this contrast microbubble into future clinical applications, such as monitoring anti-angiogenic cancer therapy.

Hybrid Molecular Acoustic Imaging: Energy in, and sound out

The photoacoustic (PA) effect was first described in 1880 by Alexander Graham Bell,[74, 75] who noted that illuminated objects emit sound waves; however, the application of the PA effect in biomedicine has not taken shape until the last decade.[75, 76] The main advantage of this molecular imaging technique is that a wide variety of contrast agents - from small molecules (e.g., dyes[77]) to nanoparticles (e.g, SWNT[45]) - can be utilized for attachment to molecular ligands (Figure 1) provided that they are highly light absorbent (Figure 6).[75] Nanoparticles and small molecules are very stable in the body; have the ability to extravasate leaky vessels; bind to targets in high densities due to their small size; and, the unbound fraction can clear from circulation relatively rapidly.[78] Furthermore, recent developments have shown that various forms of energy, including optical sources (e.g., lasers; conventional PA; also called optoacoustics),[75] radiofrequency waves (RF; also called thermoacoustics),[75] microwaves,[75, 79] and magnetic field pulses (for detection of magnetic nanoparticles with ultrasound; also called magnetoacoustics),[80, 81] can be used to result in contrast agent "activation" – meaning, the energy input heats the contrast agent causing thermal expansion and increased acoustic pressure.[75] Short pulses of energy are applied to result in time variant pressure changes, and higher signal to noise ratios.[75]

PA sensing instruments include microscopy (PAM), tomography (PAT, or thermoacoustic tomography (TAT)), spectroscopy (PAS), and flow cytometry (PAFC)[82] for high-resolution molecular imaging at surfaces, in circulation (e.g., contrast agents in blood flow (PA Doppler)[83, 84] or cells labeled with contrast agents in blood[82]), and in deep-tissues;[75] thus, PA molecular imaging techniques are promising for a wide range of micro- and macro-scaled applications (Figure 6). Strategies for detection of sound waves can be acoustic-based (e.g., use of ultrasound transducers[75]) or optical-based (e.g., a device that measures changes in thickness of an optical film as a result of acoustic pressures generated by PA[85]) and are reviewed elsewhere.[75] In addition to measuring signal from activated contrast agents, PA imaging can also be used to measure local temperature (by relating PA pressure to temperature with high, sub-degree sensitivity[86, 87]) and chemical environments, such as oxygenation[88] and pH.[89] Wang et al.[76] describes several potential applications of PA molecular imaging for clinical translation, including: 1) real-time PAM imaging as complimentary to optical-based microscopy methods (mentioned above); 2) real-time PAM imaging and/or PAM-Doppler (blood flow imaging – see Fang et al.[83]) imaging of melanoma; 3) PA endoscopy for more sensitive and early detection of gastrointestinal cancer; 4) cancer detection at the molecular level (e.g., RGD-targeted SWNTs for detection of vascularized gliomas[45]); 5) high-resolution PAT imaging of reporter genes; 6) PA Doppler flow measurements of blood velocity (more sensitive than conventional Doppler US, which suffers from noise artifacts generated by red blood cells); 7) PAT imaging of blood oxygenation; 8) real-time PAT staging of breast cancer with sentinel lymph node mapping; 9) Multiscale (i.e., both microscopic and macroscopic; Figure 6) *in vivo* imaging (compared with PET, SPECT, MRI, CT, and US, which are only used for macroscopic imaging); 10) PAT and/or TAT for high-resolution and high-specificity breast cancer diagnosis/screening to replace x-ray mammography; 11) PAT and/or TAT for functional brain imaging; and, 12) RF-TAT molecular imaging once specific RF-activated contrast agents are developed. Infinitely more applications are possible with PAM, PAT, and TAT, as more sophisticated device technology and contrast agents are developed. As with ultrasound transducers for non-invasive (abdominal, transcranial, breast) and more invasive (transvaginal, endoscopic, intravascular) imaging strategies, PAT/TAT imaging devices equipped with both contrast agent activation (e.g., optical or electromagnetic source) and acoustic pressure measurement can access most tissue. Various types of nanoparticles, including nano-rods, -cages, -spheres, -tubes, -shells, and other nanoparticles consisting of gold,[78] iron oxide,[80, 81], cobalt,[90] silica (e.g., photonic explorers for bioanalysis with

biologically localized embedding (PEBBLES)[91, 92] filled with near-infrared-red absorbing dyes, such as the FDA-approved dye, iodocyanine green (ICG); see Yang et al.[93] for review) or carbon,[45] have been tested preclinically as PA imaging contrast agents (Table 5). Furthermore, they can be easily conjugated to targeting moieties (e.g., antibodies, peptides, small molecules) for molecular imaging as well as drugs for targeted therapy.[75, 93, 94]

The advantages of PA imaging are numerous: 1) target-specific signal can be obtained without interference from background tissues (similar in respect to PET modality), and can be overlaid on top of an ultrasound anatomical image for cross-referencing with morphology (similar to PET signal overlaid on CT); 2) does not involve ionizing irradiation; 3) can visualize targeted nanoparticles with high sensitivity and resolution; and, 4) can image both on the macroscopic (with PAT imaging) and microscopic (with PAM imaging and other molecular detection methods including PA flow cytometery and spectrophotometry) levels. Additionally, PAT imaging has similar advantages to US imaging (Table 1) in that it can provide real-time, inexpensive, and quantitative molecular imaging at high resolution. This preclinical molecular imaging approach has a large potential; however, several steps are needed to fully translate PA imaging techniques (not listed in order). First, PA imaging detection hardware and computation software for real-time imaging must be integrated with clinical imaging systems. Most current preclinical devices are home-made and designed for small animal imaging; therefore, future work should focus on integrating this technology on a clinically relevant device and establishing proof-of-principle studies in small animals (for example, as for molecular ultrasound imaging as shown in Figure 5, where a clinical ultrasound machine was used to image breast cancer-bearing mice). Secondly, nanoparticles must be fully characterized for toxicity, biodistribution, and pharmacokinetics[94] to take full advantage of the highly specific and sensitive molecular imaging tool that PA represents. Thirdly, further developments in contrast agent "activation" by RF, microwaves, and magnetic fields can extend the applications limited by the minimal depth penetration of optical sources. Currently a few in-human studies have used PA techniques: 1) PA spectroscopy to measure oxygenation levels in hyper- and hypo-ventilating healthy volunteers;[95] 2) PA flow cytometry to quantify circulating melanoma cells in a stage IV melanoma patient's blood sample;[96] and 3) *in vivo* PAT imaging to examine human breast tumors to visualize tumor vascularity based on optical contrast characteristic of breast tissue.[97, 98] Further developments in instrumentation and evaluation of contrast agents for photoacoustic imaging will move toward a molecular approach in the clinic.

CONCLUSIONS

Molecular imaging can be applied to all avenues of medical imaging: early detection/ screening, diagnosis, therapy delivery/monitoring, and treatment follow-up. The current status of clinical molecular imaging is limited, with most current applications using PET and SPECT imaging, and a small number of highly specific applications for MRI/MRS, optical, and ultrasound. Current demands and trends are calling for new strategies to focus on early disease detection through improved imaging and screening protocols, as well as patient-specific treatment selection (personalized medicine), delivery (possibly through targeted therapy), and therapy-specific (i.e., therapeutic target) monitoring. It is hoped that these new strategies of early diagnosis and immediate treatment monitoring will improve success rates for curing diseases with high mortality rates such as cardiovascular disease and cancer, as well as providing more specific treatment for other diseases (for example, neurological disorders such as Alzheimers and/or Parkinsons). Preclinical research has resulted in the identification of a large number of molecular targets and the development of novel molecular imaging contrast agents as well as device, hardware, and software technologies. It is expected that molecular imaging with imaging modalities other than PET and SPECT,

including MRI/MRS, optical (Raman), molecular ultrasound and photoacoustic tomography, will be integrated into more frequent clinical use in the near future.

References

1. Mankoff DA. A definition of molecular imaging. J Nucl Med. 2007:48.

2. Peterson TE, Manning HC. Molecular imaging: 18F-FDG PET and a whole lot more. J Nucl Med Technol. 2009:37.

3. Wong ST. Emerging treatment combinations: integrating therapy into clinical practice. Am J Health Syst Pharm. 2009:66.

4. Blanco E, Kessinger CW, Sumer BD, Gao J. Multifunctional micellar nanomedicine for cancer therapy. Exp Biol Med (Maywood). 2009:234.

5. Desar IM, van Herpen CM, van Laarhoven HW, Barentsz JO, Oyen WJ, van der Graaf WT. Beyond RECIST: molecular and functional imaging techniques for evaluation of response to targeted therapy. Cancer Treat Rev. 2009:35.

6. Lucignani G. Monitoring cancer therapy with PET: probably effective, but more research is needed. Eur J Nucl Med Mol Imaging. 2009:36.

7. Serkova NJ, Hasebroock KM, Kraft SL. Magnetic resonance spectroscopy of living tissues. Methods Mol Biol. 2009:520.

8. Soares DP, Law M. Magnetic resonance spectroscopy of the brain: review of metabolites and clinical applications. Clin Radiol. 2009:64. [PubMed: 19070699]

9. van der Graaf M. In vivo magnetic resonance spectroscopy: basic methodology and clinical applications. Eur Biophys J. 2009

10. De Stefano N, Filippi M, Miller D, et al. Guidelines for using proton MR spectroscopy in multicenter clinical MS studies. Neurology. 2007:69.

11. Boesch C. Musculoskeletal spectroscopy. J Magn Reson Imaging. 2007:25.

12. Kim HL. Optical imaging in oncology. Urol Oncol. 2009:27.

13. Konig K. Clinical multiphoton tomography. J Biophotonics. 2008:1.

14. Chen J, Lee L. Clinical applications and new developments of optical coherence tomography: an evidence-based review. Clin Exp Optom. 2007:90.

15. Zysk AM, Nguyen FT, Oldenburg AL, Marks DL, Boppart SA. Optical coherence tomography: a review of clinical development from bench to bedside. J Biomed Opt. 2007:12.

16. Contag CH. In vivo pathology: seeing with molecular specificity and cellular resolution in the living body. Annu Rev Pathol. 2007:2.

17. Wang TD, Friedland S, Sahbaie P, et al. Functional imaging of colonic mucosa with a fibered confocal microscope for real-time in vivo pathology. Clin Gastroenterol Hepatol. 2007:5.

18. Konig K, Weinigel M, Hoppert D, et al. Multiphoton tissue imaging using high-NA microendoscopes and flexible scan heads for clinical studies and small animal research. J Biophotonics. 2008:1.

19. Robert B. Resonance Raman spectroscopy. Photosynth Res. 2009:101.

20. Wachsmann-Hogiu S, Weeks T, Huser T. Chemical analysis in vivo and in vitro by Raman spectroscopy--from single cells to humans. Curr Opin Biotechnol. 2009:20.

21. Motz JT, Fitzmaurice M, Miller A, et al. In vivo Raman spectral pathology of human atherosclerosis and vulnerable plaque. J Biomed Opt. 2006:11.

22. Haka AS, Volynskaya Z, Gardecki JA, et al. In vivo margin assessment during partial mastectomy breast surgery using raman spectroscopy. Cancer Res. 2006:66.

23. Huang Z, Teh SK, Zheng W, et al. Integrated Raman spectroscopy and trimodal wide-field imaging techniques for real-time in vivo tissue Raman measurements at endoscopy. Opt Lett. 2009:34. [PubMed: 19109631]

24. Kim DE, Kim JY, Schellingerhout D, et al. Protease Imaging of Human Atheromata Captures Molecular Information of Atherosclerosis, Complementing Anatomic Imaging. Arterioscler Thromb Vasc Biol. 2010

25. George A, Movahed A. Cardiac computed tomography: current practice and future applications. Rev Cardiovasc Med. 2009:10.

26. Weskott HP. Emerging roles for contrast-enhanced ultrasound. Clin Hemorheol Microcirc. 2008:40.

27. Celli N, Gaiani S, Piscaglia F, et al. Characterization of liver lesions by real-time contrast-enhanced ultrasonography. Eur J Gastroenterol Hepatol. 2007:19.

28. Wilson SR, Jang HJ, Kim TK, Iijima H, Kamiyama N, Burns PN. Real-time temporal maximum-intensity-projection imaging of hepatic lesions with contrast-enhanced sonography. AJR Am J Roentgenol. 2008:190. [PubMed: 18562745]

29. Pochon S, Tardy I, Bussat P, et al. BR55: a lipopeptide-based VEGFR2-targeted ultrasound contrast agent for molecular imaging of angiogenesis. Invest Radiol. 2010:45.

30. Pysz MA, Foygel K, Rosenberg J, Gambhir SS, Schneider M, Willmann JK. Monitoring anti-angiogenic therapy with molecular ultrasound and a new clinically translatable contrast agent (BR55). Radiology. In Press.

31. Willmann JK, van Bruggen N, Dinkelborg LM, Gambhir SS. Molecular imaging in drug development. Nat Rev Drug Discov. 2008:7.

32. Agdeppa ED, Spilker ME. A review of imaging agent development. AAPS J. 2009:11. [PubMed: 19921438]

33. Alencar H, Funovics MA, Figueiredo J, Sawaya H, Weissleder R, Mahmood U. Colonic adenocarcinomas: near-infrared microcatheter imaging of smart probes for early detection--study in mice. Radiology. 2007:244. [PubMed: 17185671]

34. Gounaris E, Tung CH, Restaino C, et al. Live imaging of cysteine-cathepsin activity reveals dynamics of focal inflammation, angiogenesis, and polyp growth. PLoS One. 2008:3.

35. Figueiredo JL, Alencar H, Weissleder R, Mahmood U. Near infrared thoracoscopy of tumoral protease activity for improved detection of peripheral lung cancer. Int J Cancer. 2006:118.

36. Jaffer FA, Vinegoni C, John MC, et al. Real-time catheter molecular sensing of inflammation in proteolytically active atherosclerosis. Circulation. 2008:118.

37. Weissleder R, Tung CH, Mahmood U, Bogdanov A Jr. In vivo imaging of tumors with protease-activated near-infrared fluorescent probes. Nat Biotechnol. 1999:17. [PubMed: 9920256]

38. Pierce MC, Javier DJ, Richards-Kortum R. Optical contrast agents and imaging systems for detection and diagnosis of cancer. Int J Cancer. 2008:123. [PubMed: 18386791]

39. Hsiung PL, Hardy J, Friedland S, et al. Detection of colonic dysplasia in vivo using a targeted heptapeptide and confocal microendoscopy. Nat Med. 2008:14. [PubMed: 18180711]

40. Liu JT, Helms MW, Mandella MJ, Crawford JM, Kino GS, Contag CH. Quantifying cell-surface biomarker expression in thick tissues with ratiometric three-dimensional microscopy. Biophys J. 2009:96.

41. Zavaleta C, de la Zerda A, Liu Z, et al. Noninvasive Raman spectroscopy in living mice for evaluation of tumor targeting with carbon nanotubes. Nano Lett. 2008:8.

42. Kneipp J, Kneipp H, Kneipp K. SERS--a single-molecule and nanoscale tool for bioanalytics. Chem Soc Rev. 2008:37.

43. Zavaleta CL, Smith BR, Walton I, et al. Multiplexed imaging of surface enhanced Raman scattering nanotags in living mice using noninvasive Raman spectroscopy. Proc Natl Acad Sci U S A. 2009:106.

44. Muller M, Zumbusch A. Coherent anti-Stokes Raman Scattering Microscopy. Chemphyschem. 2007:8.

45. De la Zerda A, Zavaleta C, Keren S, et al. Carbon nanotubes as photoacoustic molecular imaging agents in living mice. Nat Nanotechnol. 2008:3.

46. Dijkstra RJ, Scheenen WJ, Dam N, Roubos EW, ter Meulen JJ. Monitoring neurotransmitter release using surface-enhanced Raman spectroscopy. J Neurosci Methods. 2007:159. [PubMed: 17706788]

47. Wang Z, Bonoiu A, Samoc M, Cui Y, Prasad PN. Biological pH sensing based on surface enhanced Raman scattering through a 2-aminothiophenol-silver probe. Biosens Bioelectron. 2008:23.

48. Evans CL, Potma EO, Puoris'haag M, Cote D, Lin CP, Xie XS. Chemical imaging of tissue in vivo with video-rate coherent anti-Stokes Raman scattering microscopy. Proc Natl Acad Sci U S A. 2005:102.

49. Huff TB, Cheng JX. In vivo coherent anti-Stokes Raman scattering imaging of sciatic nerve tissue. J Microsc. 2007:225.

50. Kaufmann BA. Ultrasound molecular imaging of atherosclerosis. Cardiovasc Res. 2009:83. [PubMed: 19497962]

51. Lindner JR. Molecular imaging of cardiovascular disease with contrast-enhanced ultrasonography. Nat Rev Cardiol. 2009:6.

52. Hwang M, Niermann KJ, Lyshchik A, Fleischer AC. Sonographic assessment of tumor response: from in vivo models to clinical applications. Ultrasound Q. 2009:25.

53. Strobel D, Seitz K, Blank W, et al. Tumor-specific vascularization pattern of liver metastasis, hepatocellular carcinoma, hemangioma and focal nodular hyperplasia in the differential diagnosis of 1,349 liver lesions in contrast-enhanced ultrasound (CEUS). Ultraschall Med. 2009:30.

54. Kaufmann BA, Sanders JM, Davis C, et al. Molecular imaging of inflammation in atherosclerosis with targeted ultrasound detection of vascular cell adhesion molecule-1. Circulation. 2007:116.

55. Lindner JR. Contrast ultrasound molecular imaging of inflammation in cardiovascular disease. Cardiovasc Res. 2009:84. [PubMed: 19150977]

56. Klibanov AL. Preparation of targeted microbubbles: ultrasound contrast agents for molecular imaging. Med Biol Eng Comput. 2009:47.

57. Marshall D, Pedley RB, Boden JA, Boden R, Melton RG, Begent RH. Polyethylene glycol modification of a galactosylated streptavidin clearing agent: effects on immunogenicity and clearance of a biotinylated anti-tumour antibody. Br J Cancer. 1996:73.

58. Willmann JK, Lutz AM, Paulmurugan R, et al. Dual-targeted contrast agent for US assessment of tumor angiogenesis in vivo. Radiology. 2008:248.

59. Willmann JK, Paulmurugan R, Chen K, et al. US imaging of tumor angiogenesis with microbubbles targeted to vascular endothelial growth factor receptor type 2 in mice. Radiology. 2008:246.

60. Palmowski M, Huppert J, Ladewig G, et al. Molecular profiling of angiogenesis with targeted ultrasound imaging: early assessment of antiangiogenic therapy effects. Mol Cancer Ther. 2008:7.

61. Korpanty G, Carbon JG, Grayburn PA, Fleming JB, Brekken RA. Monitoring response to anticancer therapy by targeting microbubbles to tumor vasculature. Clin Cancer Res. 2007:13.

62. Lee DJ, Lyshchik A, Huamani J, Hallahan DE, Fleischer AC. Relationship between retention of a vascular endothelial growth factor receptor 2 (VEGFR2)-targeted ultrasonographic contrast agent and the level of VEGFR2 expression in an in vivo breast cancer model. J Ultrasound Med. 2008:27.

63. Rychak JJ, Graba J, Cheung AM, et al. Microultrasound molecular imaging of vascular endothelial growth factor receptor 2 in a mouse model of tumor angiogenesis. Mol Imaging. 2007:6.

64. Lyshchik A, Fleischer AC, Huamani J, Hallahan DE, Brissova M, Gore JC. Molecular imaging of vascular endothelial growth factor receptor 2 expression using targeted contrast-enhanced high-frequency ultrasonography. J Ultrasound Med. 2007:26.

65. Willmann JK, Kimura RH, Deshpande N, Lutz AM, Cochran JR, Gambhir SS. Targeted Contrast-Enhanced Ultrasound Imaging of Tumor Angiogenesis with Contrast Microbubbles Conjugated to Integrin-Binding Knottin Peptides. J Nucl Med. 2010

66. Bachmann C, Klibanov AL, Olson TS, et al. Targeting mucosal addressin cellular adhesion molecule (MAdCAM)-1 to noninvasively image experimental Crohn's disease. Gastroenterology. 2006:130. [PubMed: 16831597]

67. Kaufmann BA, Carr CL, Belcik JT, et al. Molecular imaging of the initial inflammatory response in atherosclerosis: implications for early detection of disease. Arterioscler Thromb Vasc Biol. 2010:30.

68. Barreiro O, Aguilar RJ, Tejera E, et al. Specific targeting of human inflamed endothelium and in situ vascular tissue transfection by the use of ultrasound contrast agents. JACC Cardiovasc Imaging. 2009:2.

69. Reinhardt M, Hauff P, Linker RA, et al. Ultrasound derived imaging and quantification of cell adhesion molecules in experimental autoimmune encephalomyelitis (EAE) by Sensitive Particle Acoustic Quantification (SPAQ). Neuroimage. 2005:27.

70. Weller GE, Lu E, Csikari MM, et al. Ultrasound imaging of acute cardiac transplant rejection with microbubbles targeted to intercellular adhesion molecule-1. Circulation. 2003:108. [PubMed: 14662713]

71. Kaufmann BA, Lewis C, Xie A, Mirza-Mohd A, Lindner JR. Detection of recent myocardial ischaemia by molecular imaging of P-selectin with targeted contrast echocardiography. Eur Heart J. 2007:28.

72. Lindner JR, Song J, Christiansen J, Klibanov AL, Xu F, Ley K. Ultrasound assessment of inflammation and renal tissue injury with microbubbles targeted to P-selectin. Circulation. 2001:104.

73. Villanueva FS, Lu E, Bowry S, et al. Myocardial ischemic memory imaging with molecular echocardiography. Circulation. 2007:115.

74. Bell AG. The Production of Sound by Radiant Energy. Science. 1881:2.

75. Li C, Wang LV. Photoacoustic tomography and sensing in biomedicine. Phys Med Biol. 2009:54.

76. Wang LV. Prospects of photoacoustic tomography. Med Phys. 2008:35.

77. Razansky D, Baeten J, Ntziachristos V. Sensitivity of molecular target detection by multispectral optoacoustic tomography (MSOT). Med Phys. 2009:36.

78. Yang X, Stein EW, Ashkenazi S, Wang LV. Nanoparticles for photoacoustic imaging. Wiley Interdiscip Rev Nanomed Nanobiotechnol. 2009:1.

79. Jin X, Li C, Wang LV. Effects of acoustic heterogeneities on transcranial brain imaging with microwave-induced thermoacoustic tomography. Med Phys. 2008:35.

80. Mehrmohammadi M, Oh J, Aglyamov SR, Karpiouk AB, Emelianov SY. Pulsed magneto-acoustic imaging. Conf Proc IEEE Eng Med Biol Soc. 2009:1. [PubMed: 19963704]

81. Qu M, Mallidi S, Mehrmohammadi M, et al. Combined photoacoustic and magneto-acoustic imaging. Conf Proc IEEE Eng Med Biol Soc. 2009:1. [PubMed: 19963704]

82. Zharov VP, Galanzha EI, Tuchin VV. In vivo photothermal flow cytometry: imaging and detection of individual cells in blood and lymph flow. J Cell Biochem. 2006:97.

83. Fang H, Maslov K, Wang LV. Photoacoustic Doppler effect from flowing small light-absorbing particles. Phys Rev Lett. 2007:99.

84. Fang H, Wang LV. M-mode photoacoustic particle flow imaging. Opt Lett. 2009:34. [PubMed: 19109631]

85. Zhang E, Laufer J, Beard P. Backward-mode multiwavelength photoacoustic scanner using a planar Fabry-Perot polymer film ultrasound sensor for high-resolution three-dimensional imaging of biological tissues. Appl Opt. 2008:47.

86. Shah J, Aglyamov SR, Sokolov K, Milner TE, Emelianov SY. Ultrasound imaging to monitor photothermal therapy - feasibility study. Opt Express. 2008:16.

87. Shah J, Park S, Aglyamov S, et al. Photoacoustic imaging and temperature measurement for photothermal cancer therapy. J Biomed Opt. 2008:13.

88. Ashkenazi S, Huang SW, Horvath T, Koo YE, Kopelman R. Photoacoustic probing of fluorophore excited state lifetime with application to oxygen sensing. J Biomed Opt. 2008:13.

89. Horvath TD, Kim G, Kopelman R, Ashkenazi S. Ratiometric photoacoustic sensing of pH using a "sonophore". Analyst. 2008:133. [PubMed: 18087624]

90. Bouchard LS, Anwar MS, Liu GL, et al. Picomolar sensitivity MRI and photoacoustic imaging of cobalt nanoparticles. Proc Natl Acad Sci U S A. 2009:106.

91. Buck SM, Koo YE, Park E, et al. Optochemical nanosensor PEBBLEs: photonic explorers for bioanalysis with biologically localized embedding. Curr Opin Chem Biol. 2004:8. [PubMed: 15036150]

92. Buck SM, Xu H, Brasuel M, Philbert MA, Kopelman R. Nanoscale probes encapsulated by biologically localized embedding (PEBBLEs) for ion sensing and imaging in live cells. Talanta. 2004:63.

93. Yang JM, Maslov K, Yang HC, Zhou Q, Shung KK, Wang LV. Photoacoustic endoscopy. Opt Lett. 2009:34. [PubMed: 19109631]

94. Fadeel B, Garcia-Bennett AE. Better safe than sorry: Understanding the toxicological properties of inorganic nanoparticles manufactured for biomedical applications. Adv Drug Deliv Rev. 2009

95. Cavaliere F, Volpe C, Gargaruti R, et al. Effects of acute hypoventilation and hyperventilation on exhaled carbon monoxide measurement in healthy volunteers. BMC Pulm Med. 2009:9. [PubMed: 19226451]

96. Weight RM, Dale PS, Viator JA. Detection of circulating melanoma cells in human blood using photoacoustic flowmetry. Conf Proc IEEE Eng Med Biol Soc. 2009:1. [PubMed: 19963704]

97. Ermilov SA, Khamapirad T, Conjusteau A, et al. Laser optoacoustic imaging system for detection of breast cancer. J Biomed Opt. 2009:14.

98. Manohar S, Vaartjes SE, van Hespen JC, et al. Initial results of in vivo non-invasive cancer imaging in the human breast using near-infrared photoacoustics. Opt Express. 2007:15.

99. Keren S, Zavaleta C, Cheng Z, de la Zerda A, Gheysens O, Gambhir SS. Noninvasive molecular imaging of small living subjects using Raman spectroscopy. Proc Natl Acad Sci U S A. 2008:105.

100. Song KH, Kim C, Maslov K, Wang LV. Noninvasive in vivo spectroscopic nanorod-contrast photoacoustic mapping of sentinel lymph nodes. Eur J Radiol. 2009:70.

101. Sinusas AJ, Bengel F, Nahrendorf M, et al. Multimodality cardiovascular molecular imaging, part I. Circ Cardiovasc Imaging. 2008:1.

102. Ng CS, Wang X, Faria SC, Lin E, Charnsangavej C, Tannir NM. Perfusion CT in patients with metastatic renal cell carcinoma treated with interferon. AJR Am J Roentgenol. 2010:194. [PubMed: 20566816]

103. Margolis DJ, Hoffman JM, Herfkens RJ, Jeffrey RB, Quon A, Gambhir SS. Molecular imaging techniques in body imaging. Radiology. 2007:245. [PubMed: 17885192]

104. Goldsmith SJ. Radioimmunotherapy of lymphoma: bexxar and zevalin. Semin Nucl Med. 2010:40.

105. Mariani G, Bruselli L, Kuwert T, et al. A review on the clinical uses of SPECT/CT. Eur J Nucl Med Mol Imaging. 2010

106. Harisinghani MG, Barentsz J, Hahn PF, et al. Noninvasive detection of clinically occult lymph-node metastases in prostate cancer. N Engl J Med. 2003:348.

107. Harisinghani MG, Jhaveri KS, Weissleder R, et al. MRI contrast agents for evaluating focal hepatic lesions. Clin Radiol. 2001:56.

108. Al-Mallah M, Kwong RY. Clinical application of cardiac CMR. Rev Cardiovasc Med. 2009:10.

109. Blamek S, Larysz D, Ficek K, Sokol M, Miszczyk L, Tarnawski R. MR spectroscopic evaluation of brain tissue damage after treatment for pediatric brain tumors. Acta Neurochir Suppl. 2010:106.

110. Modrego PJ, Pina MA, Fayed N, Diaz M. Changes in metabolite ratios after treatment with rivastigmine in Alzheimer's disease: a nonrandomised controlled trial with magnetic resonance spectroscopy. CNS Drugs. 2006:20.

111. Schnell GB, Kryski AJ, Mann L, Anderson TJ, Belenkie I. Contrast echocardiography accurately predicts myocardial perfusion before angiography during acute myocardial infarction. Can J Cardiol. 2007:23.

112. Jang IK, Tearney GJ, MacNeill B, et al. In vivo characterization of coronary atherosclerotic plaque by use of optical coherence tomography. Circulation. 2005:111.

113. Lieber CA, Majumder SK, Ellis DL, Billheimer DD, Mahadevan-Jansen A. In vivo nonmelanoma skin cancer diagnosis using Raman microspectroscopy. Lasers Surg Med. 2008:40.

114. Massoud TF, Gambhir SS. Molecular imaging in living subjects: seeing fundamental biological processes in a new light. Genes Dev. 2003:17.

115. Mercer JR. Molecular imaging agents for clinical positron emission tomography in oncology other than fluorodeoxyglucose (FDG): applications, limitations and potential. J Pharm Pharm Sci. 2007:10.

116. Dunphy MP, Lewis JS. Radiopharmaceuticals in preclinical and clinical development for monitoring of therapy with PET. J Nucl Med. 2009; 50(Suppl 1)

117. Mittra E, Quon A. Positron emission tomography/computed tomography: the current technology and applications. Radiol Clin North Am. 2009:47.

118. Lalonde L, Ziadi MC, Beanlands R. Cardiac positron emission tomography: current clinical practice. Cardiol Clin. 2009:27.

119. Wang J, Maurer L. Positron Emission Tomography: applications in drug discovery and drug development. Curr Top Med Chem. 2005:5.

120. Parsey RV, Mann JJ. Applications of positron emission tomography in psychiatry. Semin Nucl Med. 2003:33.

121. Pantaleo MA, Nannini M, Maleddu A, et al. Conventional and novel PET tracers for imaging in oncology in the era of molecular therapy. Cancer Treat Rev. 2008:34.

122. Josephs D, Spicer J, O'Doherty M. Molecular imaging in clinical trials. Target Oncol. 2009:4.

123. Liu S. The role of coordination chemistry in the development of target-specific radiopharmaceuticals. Chem Soc Rev. 2004:33.

124. Lampl Y, Lorberboym M, Blankenberg FG, Sadeh M, Gilad R. Annexin V SPECT imaging of phosphatidylserine expression in patients with dementia. Neurology. 2006:66.

125. Burtscher IM, Holtas S. Proton MR spectroscopy in clinical routine. J Magn Reson Imaging. 2001:13.

126. Beloueche-Babari M, Chung YL, Al-Saffar NM, Falck-Miniotis M, Leach MO. Metabolic assessment of the action of targeted cancer therapeutics using magnetic resonance spectroscopy. Br J Cancer. 2010:102.

127. Kurhanewicz J, Bok R, Nelson SJ, Vigneron DB. Current and potential applications of clinical 13C MR spectroscopy. J Nucl Med. 2008:49.

128. Molckovsky A, Song LM, Shim MG, Marcon NE, Wilson BC. Diagnostic potential of near-infrared Raman spectroscopy in the colon: differentiating adenomatous from hyperplastic polyps. Gastrointest Endosc. 2003:57.

129. Blankenberg FG. In vivo imaging of apoptosis. Cancer Biol Ther. 2008:7.

130. Gangloff A, Hsueh WA, Kesner AL, et al. Estimation of paclitaxel biodistribution and uptake in human-derived xenografts in vivo with (18)F-fluoropaclitaxel. J Nucl Med. 2005:46.

131. van Tilborg GA, Mulder WJ, Chin PT, et al. Annexin A5-conjugated quantum dots with a paramagnetic lipidic coating for the multimodal detection of apoptotic cells. Bioconjug Chem. 2006:17.

132. Yu KN, Lee SM, Han JY, et al. Multiplex targeting, tracking, and imaging of apoptosis by fluorescent surface enhanced Raman spectroscopic dots. Bioconjug Chem. 2007:18.

133. Mishani E, Hagooly A. Strategies for molecular imaging of epidermal growth factor receptor tyrosine kinase in cancer. J Nucl Med. 2009:50.

134. Mankoff DA, Link JM, Linden HM, Sundararajan L, Krohn KA. Tumor receptor imaging. J Nucl Med. 2008; 49(Suppl 2)

135. Xu N, Cai G, Ye W, et al. Molecular imaging application of radioiodinated anti-EGFR human Fab to EGFR-overexpressing tumor xenografts. Anticancer Res. 2009:29.

136. Li PC, Wang CR, Shieh DB, et al. In vivo photoacoustic molecular imaging with simultaneous multiple selective targeting using antibody-conjugated gold nanorods. Opt Express. 2008:16.

137. Kah JC, Kho KW, Lee CG, et al. Early diagnosis of oral cancer based on the surface plasmon resonance of gold nanoparticles. Int J Nanomedicine. 2007:2.

138. Niu G, Cai W, Chen X. Molecular imaging of human epidermal growth factor receptor 2 (HER-2) expression. Front Biosci. 2008:13.

139. Bhattacharyya S, Wang S, Reinecke D, Kiser W Jr, Kruger RA, DeGrado TR. Synthesis and evaluation of near-infrared (NIR) dye-herceptin conjugates as photoacoustic computed tomography (PCT) probes for HER2 expression in breast cancer. Bioconjug Chem. 2008:19.

140. Sha MY, Xu H, Natan MJ, Cromer R. Surface-enhanced Raman scattering tags for rapid and homogeneous detection of circulating tumor cells in the presence of human whole blood. J Am Chem Soc. 2008:130.

141. Kang B, Yu D, Dai Y, Chang S, Chen D, Ding Y. Cancer-cell targeting and photoacoustic therapy using carbon nanotubes as "bomb" agents. Small. 2009:5.

142. Ljungkvist AS, Bussink J, Kaanders JH, van der Kogel AJ. Dynamics of tumor hypoxia measured with bioreductive hypoxic cell markers. Radiat Res. 2007:167. [PubMed: 17390724]

143. Reischl G, Dorow DS, Cullinane C, et al. Imaging of tumor hypoxia with [124I]IAZA in comparison with [18F]FMISO and [18F]FAZA--first small animal PET results. J Pharm Pharm Sci. 2007:10.

144. Krohn KA, Link JM, Mason RP. Molecular imaging of hypoxia. J Nucl Med. 2008; 49(Suppl 2)

145. Lungu GF, Li ML, Xie X, Wang LV, Stoica G. In vivo imaging and characterization of hypoxia-induced neovascularization and tumor invasion. Int J Oncol. 2007:30.

146. Shah NC, Lyandres O, Walsh JT Jr, Glucksberg MR, Van Duyne RP. Lactate and sequential lactate-glucose sensing using surface-enhanced Raman spectroscopy. Anal Chem. 2007:79. [PubMed: 17194124]

147. Cai W, Chen X. Multimodality molecular imaging of tumor angiogenesis. J Nucl Med. 2008; 49(Suppl 2)

148. Cai W, Gambhir SS, Chen X. Chapter 7 Molecular imaging of tumor vasculature. Methods Enzymol. 2008:445.

149. Miao Z, Ren G, Liu H, et al. An engineered knottin peptide labeled with 18F for PET imaging of integrin expression. Bioconjug Chem. 2009:20. [PubMed: 19099498]

150. Wang L, Xie X, Oh JT, et al. Combined photoacoustic and molecular fluorescence imaging in vivo. Conf Proc IEEE Eng Med Biol Soc. 2005:1. [PubMed: 17282096]

151. von Forstner C, Egberts JH, Ammerpohl O, et al. Gene expression patterns and tumor uptake of 18F-FDG, 18F-FLT, and 18F-FEC in PET/MRI of an orthotopic mouse xenotransplantation model of pancreatic cancer. J Nucl Med. 2008:49.

152. Cheng Z, Levi J, Xiong Z, et al. Near-infrared fluorescent deoxyglucose analogue for tumor optical imaging in cell culture and living mice. Bioconjug Chem. 2006:17.

153. Scherer RL, McIntyre JO, Matrisian LM. Imaging matrix metalloproteinases in cancer. Cancer Metastasis Rev. 2008:27.

154. Wagner S, Breyholz HJ, Faust A, et al. Molecular imaging of matrix metalloproteinases in vivo using small molecule inhibitors for SPECT and PET. Curr Med Chem. 2006:13.

155. Jastrzebska B, Lebel R, Therriault H, et al. New enzyme-activated solubility-switchable contrast agent for magnetic resonance imaging: from synthesis to in vivo imaging. J Med Chem. 2009:52.

156. Elsasser-Beile U, Reischl G, Wiehr S, et al. PET imaging of prostate cancer xenografts with a highly specific antibody against the prostate-specific membrane antigen. J Nucl Med. 2009:50.

157. Hillier SM, Maresca KP, Femia FJ, et al. Preclinical evaluation of novel glutamate-urea-lysine analogues that target prostate-specific membrane antigen as molecular imaging pharmaceuticals for prostate cancer. Cancer Res. 2009:69.

158. Kularatne SA, Zhou Z, Yang J, Post CB, Low PS. Design, synthesis, and preclinical evaluation of prostate-specific membrane antigen targeted (99m)Tc-radioimaging agents. Mol Pharm. 2009:6.

159. Serda RE, Adolphi NL, Bisoffi M, Sillerud LO. Targeting and cellular trafficking of magnetic nanoparticles for prostate cancer imaging. Mol Imaging. 2007:6.

160. Chen Y, Dhara S, Banerjee SR, et al. A low molecular weight PSMA-based fluorescent imaging agent for cancer. Biochem Biophys Res Commun. 2009:390.

161. Gao X, Cui Y, Levenson RM, Chung LW, Nie S. In vivo cancer targeting and imaging with semiconductor quantum dots. Nat Biotechnol. 2004:22.

162. Gilad AA, Ziv K, McMahon MT, van Zijl PC, Neeman M, Bulte JW. MRI reporter genes. J Nucl Med. 2008:49.

163. Serganova I, Mayer-Kukuck P, Huang R, Blasberg R. Molecular imaging: reporter gene imaging. Handb Exp Pharmacol. 2008

164. Li L, Zhang HF, Zemp RJ, Maslov K, Wang L. Simultaneous imaging of a lacZ-marked tumor and microvasculature morphology in vivo by dual-wavelength photoacoustic microscopy. J Innov Opt Health Sci. 2008:1.
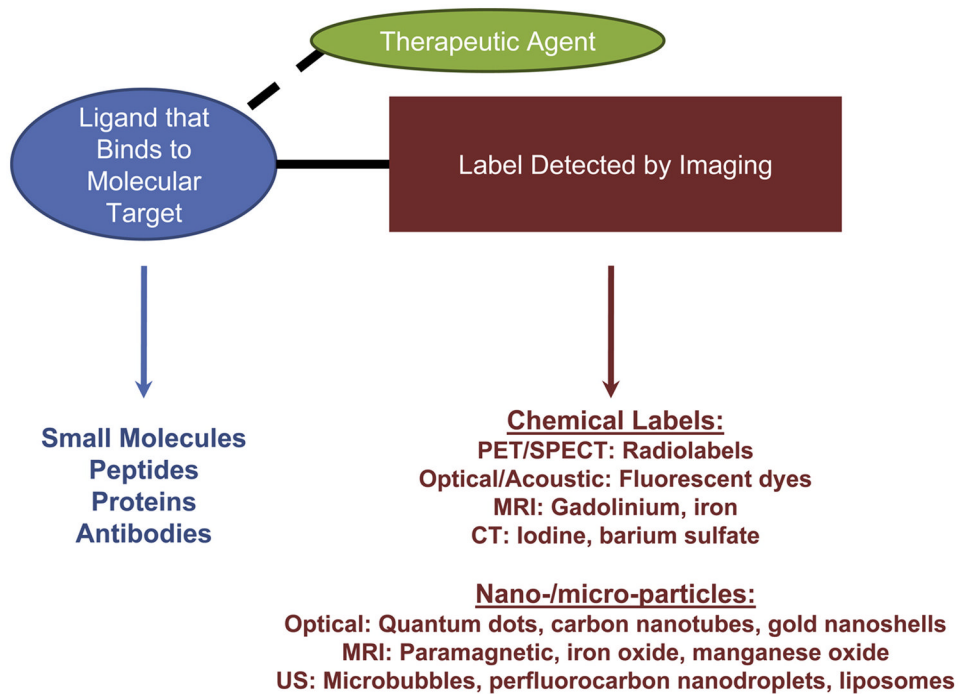
Figure 1.
Contrast agents used for molecular imaging are composed of at least 2 entities: one component such as an antibody, peptide, nucleic acid, or a small molecule for binding to the molecular target, and a label for readout by an imaging modality (see also Table 1). More sophisticated contrast agents can include multiple parts for targeting several molecules at once, as well as, several labels for multimodality imaging. Drugs can also be attached/encapsulated for targeted therapy.
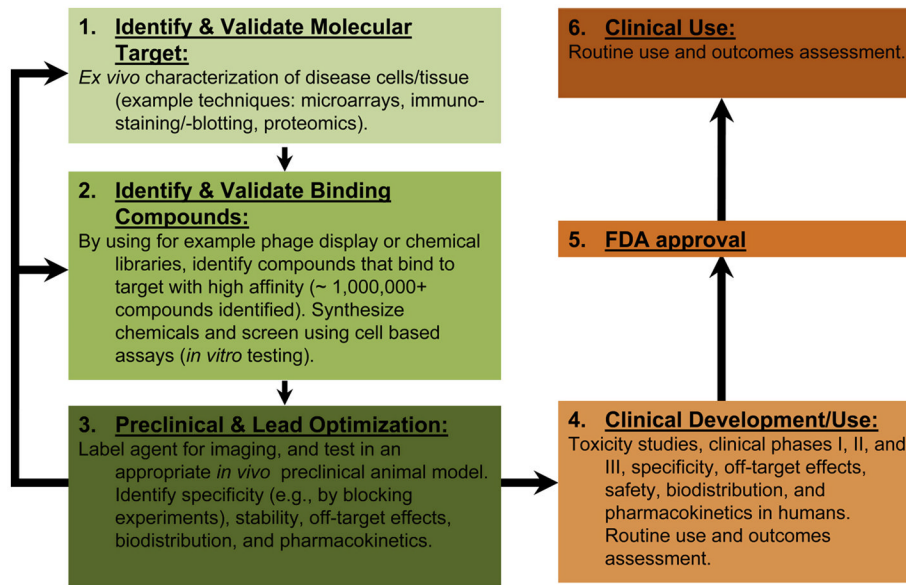
Figure 2.
Molecular contrast agent design and clinical use involve a series of steps similar to those used in drug development (Adapted from Willmann et al.[31]). Preclinical steps (green-shaded boxes) involve target identification, validation, chemical labeling, *in vitro* cellular characterization, and *in vivo* animal testing. After many optimization steps (arrows between boxes 1, 2, and 3), the agent can be tested in humans after FDA applications for investigatory new drug (IND) or exploratory IND (eIND). Clinical testing (orange boxes) involves rigorous testing for agent properties (effectiveness, specificity, toxicity, off-target effects, kinetics, etc.) before potential approval by the FDA for routine clinical use, which is also heavily monitored for outcomes assessment.
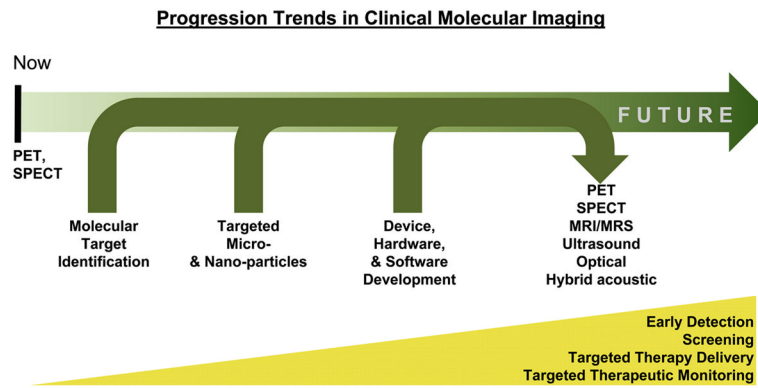
Figure 3.
Timeline representation of current and future utilization of molecular imaging in the clinic. Current approved molecular imaging techniques are mostly PET and SPECT, which are expected to continue for use in diagnosing advanced stage diseases. With a plethora of molecular targets identified preclinically for various diseases (e.g., cancer: Table 5) and advances in material engineering for nano- and micro-particle contrast agents, a large potential exists to expand clinical molecular imaging beyond nuclear medicine approaches. Molecular imaging techniques that do not expose patients to ionizing irradiation, such as MRI/MRS, optical, ultrasound and hybrid acoustic imaging approaches are ideal for early disease detection and screening. Hardware and software implementations for sensitive and quantitative detection of targeted contrast agents will also pave the way for targeted therapeutic delivery (tracking) and response monitoring. Optical, ultrasound, and hybrid acoustic imaging are expected to be forerunners in screening methodology since they can provide real-time, inexpensive, and high-resolution images.
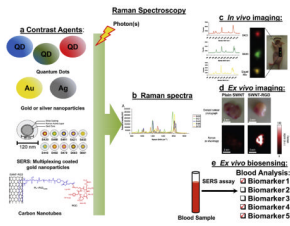
Figure 4.
Raman Spectroscopy/Microscopy techniques are an emerging molecular imaging tool for potential translation to clinical applications with endoscopes or catheters. Left to right: Nanoparticles with specific Raman signatures (*a*), including quantum dots, metal (gold (Au) or silver (Ag)) nanoparticles which can be coated for several different spectra (e.g., SERS nanoparticles such as silica coated gold nanoparticles), and carbon nanotubes/fullerenes, can be used for attaching specific moieties to bind to molecular targets (as in Figure 1 where the label is the nanoparticle). The nanoparticles (when excited with an optical laser) produce specific Raman spectra (*b*), which can be used to generate *in vivo* imaging signal (*c*), *ex vivo* imaging signal (*d*), and for *ex vivo* biosensing assays (*e*). Image in (*c*) represents *in vivo* imaging of SERS nanoparticles (S421 and S441) injected subcutaneously in nude mice, and the spectra obtained for S421, S441, and an equal mix of both S421 and S441. Reprinted with permission from Keren et al.[99] Image in (*d*) represents *ex vivo* Raman imaging of excised subcutaneous tumor xenografts that were pre-injected (in mouse prior to euthanization) with either plain, non-targeted single-walled carbon nanotubes (Plain SWNT) or SWNT's conjugated to RGD peptide (binds to $\alpha_V\beta_3$ integrin); note that RGD-targeted SWNTs show high Raman signal compared to non-targeted, plain SWNTs. SWNT structure and Raman image were reprinted with permission from de la Zerda et al.[45] Image in (*e*) represents a schematic for using Raman Spectroscopy for analyzing blood samples with nanoparticles (*a*) targeted to specific biomarkers (DNA, RNA, or proteins); this technique can be advantageous for ultrasensitive, rapid screening for early detection of cancer. Not shown: Raman imaging can also be used for resolution microscopy (e.g., CARS).
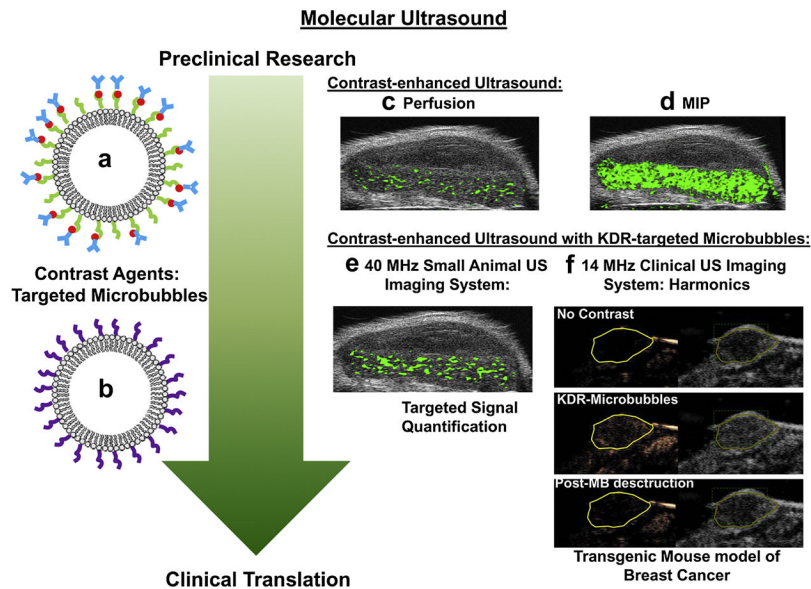
Figure 5.
Contrast-enhanced ultrasound imaging with molecularly-targeted microbubbles (MBs; molecular ultrasound imaging) is moving rapidly towards clinical translation. Left to right: Proof-of-principle preclinical studies include testing targeted MBs constructed by conjugating an antibody (blue "Y" molecule) to a MB using strept(avidin)-biotin (green line-red circle) binding chemistry (*a*) for endothelial cell target specificity and validation. Then, MBs using peptides (purple lines) with high binding affinity for the human targets can be constructed with direct conjugation to lipid MB shell (*b*), and after further rounds of preclinical testing (see Figure 2), peptide-conjugated MBs can progress to clinical testing. Functional ultrasound imaging methods including perfusion analysis with assessment of first-pass time-intensity curves (*c*) and maximum intensity persistence (MIP) (*d*) can provide levels of tissue vascularity. Molecular ultrasound imaging with KDR-targeted MBs [30] can be used to measure KDR expression levels (*e*; for more details on calculating the attached MB signal, refer to Willmann et al.[59]). (*f*) A clinical ultrasound system was used to acquire B-mode images (right side) and contrast images (see Deshpande et al. in this issue for a more detailed review of contrast imaging) of breast cancer in a transgenic mouse model.
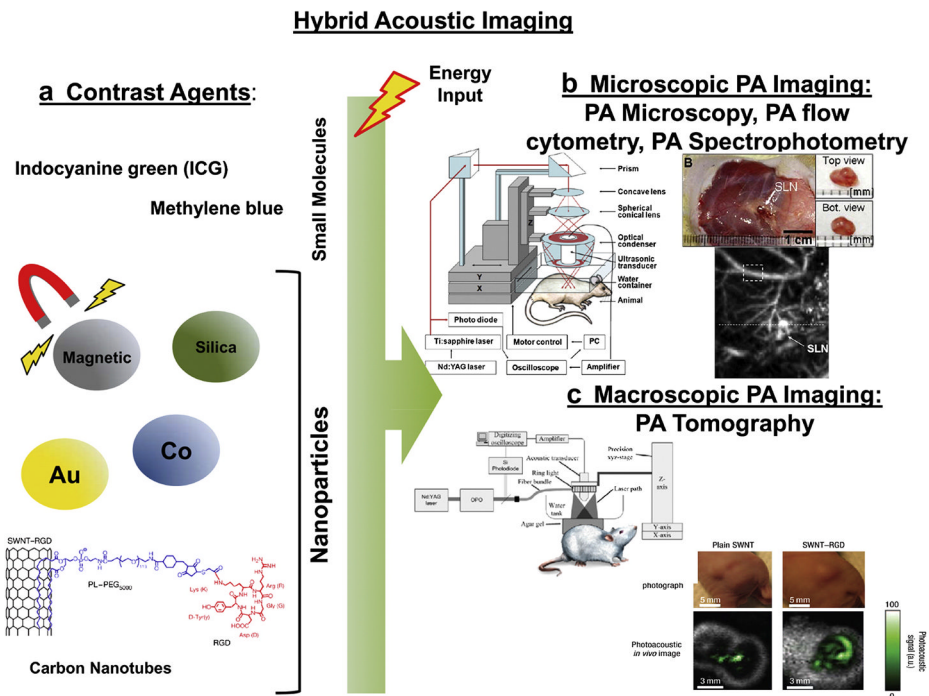
Figure 6.
Photoacoustic (PA), thermoacoustic, and magnetoacoustic imaging techniques are emerging as a highly sensitive and versatile tool for molecular imaging. Left to right: Contrast agents for use with hybrid acoustic imaging methods are optically-absorbing nanoparticles, such as small molecule dyes, nanoparticles made of silica, gold, or cobalt, and carbon nanotubes/fullerenes, for use with photoacoustic imaging; and, magnetic nanoparticles for use with magnetoacoustic imaging. Energy is applied to the nanoparticles in the form of near-infrared light, radiofrequency, microwaves, or magnetic field; this energy causes the contrast agent nanoparticles (*a*) to oscillate and produce sound waves for measurement with ultrasound. PA imaging devices have been developed for imaging at the microscale (*b*), and macroscale (*c*) levels. *In vivo* and *in vitro* micromolecular analyses can be performed with PA imaging devices such as PA microscopy, PA flow cytometry, and PA spectrophotometry (*b*). Image represents an *in vivo* PA spectrophotometry system used to image surrounding vascularity and sentinal lymph node with gold nanorods (activated with 807 nm laser) in male rats (Reprinted with permission from Song et al.[100]). Macromolecular analyses can be performed with PA tomography for *in vivo* imaging applications (*c*). Images (reprinted with permission from de la Zerda et al.[45]) represent the device setup of a PA imaging system for small animals; this system was used to generate the adjacent, lower right image of subcutaneous glioma tumor xenografts in nude mice. Plain (non-targeted)- or RGD- (targeting $\alpha_V\beta_3$ integrin) single-walled carbon nanotubes (*a*) were injected in the mouse tail vein, and PA signal (green) was imaged with B-mode US imaging (grey).

Table 1

Advantages and disadvantages of imaging modalities used with molecularly targeted or non-targeted contrast agents in a clinical setting. Adapted from references:[31, 101]

Modality	Advantages	Disadvantages	Common Contrast agents/Readout	Example Clinical Applications
CT	• Unlimited depth penetration • High spatial resolution • Whole-body imaging possible • Short acquisition time (minutes) • Moderately expensive • Anatomical imaging	• Irradiation exposure • Poor soft tissue contrast • Probably not used for molecular imaging – currently only anatomical and functional imaging	• barium • iodine • krypton • xenon	• Tumor perfusion[102]
PET	• Unlimited depth penetration • Whole-body imaging possible • Quantitative molecular imaging • Can be combined with CT or MRI for anatomical information	• Irradiation exposure • Expensive • Low spatial resolution (1–2 mm; 4–8 mm^3) • Long acquisition times (minutes to hour)	• ^{11}C • ^{18}F • ^{64}Cu • ^{68}Ga	• ^{18}F-FDG-PET for cancer staging [103] • Diagnosis of various diseases (see Table 2)
SPECT	• Unlimited depth penetration • Whole-body imaging possible • Quantitative molecular imaging • Theranostic: Can combine imaging & radiotherapy • Can be combined with CT for anatomical information	• Irradiation exposure • Low spatial resolution (0.3–1 mm; 12–15 mm^3) • Long acquisition time	• ^{99m}Tc • ^{123}I • ^{111}In • ^{177}Lu	• Diagnosis of various diseases (see Table 3) • Radiotherapy for NHL: ^{90}Y-Bexxar or ^{131}I-Zevalin[104] • Radiotherapy of thyroid carcinoma with ^{131}I-iodide[105]
MRI	• Unlimited depth penetration	• Expensive • Long acquisition	• Gadolinium (Gd^{3+}) • iron oxide particles (SPIO, USPIO)	• SPIOs for detection of lymph node

Modality	Advantages	Disadvantages	Common Contrast agents/Readout	Example Clinical Applications
	• Whole-body imaging possible • No ionizing irradiation • Excellent soft tissue contrast • High spatial resolution	time (min-hours) • Limited sensitivity for detection of molecular contrast agents	• manganese oxide • [19]F	metastases of prostate cancer[106] • Characterization of focal hepatic lesions[107] • Perfusion imaging of the heart[108]
MRS	• Whole-body imaging possible • No ionizing irradiation	• Expensive • Long acquisition time (min-hours) • Low sensitivity	• choline • creatine • lactate • lipids • polyamines • N-acetyl-aspartate	• Metabolite levels in brain tumors [109] • Treatment monitoring of Alzheimers[110]
US	• No ionizing irradiation • Real-time imaging/ short acquisition time (min) • High spatial resolution • Can be applied externally or internally (endoscopy) • Inexpensive • Highly sensitive	• Whole-body imaging not possible • Contrast agents currently limited to vasculature • Operator dependency	• Contrast Microbubbles	• Characterization of focal liver lesions[28] • Echocardiography[111] • Tumor perfusion of cancer[27]
Optical	• No ionizing irradiation • Real-time imaging/ short acquisition time (sec-min) • Relatively high spatial resolution • Can be applied externally or internally (endoscopy) • Inexpensive • Highly quantitative & sensitive	• Limited depth penetration (≤ 1 cm) • Whole-body imaging not possible	• Fluorescent molecules & dyes • Light absorbing nanoparticles	• OCT imaging of artherosclerosis[112] • OCT imaging for colonoscopy screening[17] • Raman imaging of skin cancer[113]

Modality	Advantages	Disadvantages	Common Contrast agents/Readout	Example Clinical Applications
	• Multiplexing			

Table 2

Commonly used PET tracers for clinical molecular imaging of diseases. Adapted from references:[114–122]

Medical Imaging	Molecular Target	Radiotracer(s)	Clinical Applications
Oncological Imaging	Protein synthesis	^{11}C Methionone,	Protein synthesis in tumors
	Glucose transporter	^{11}C-DG, ^{18}F-FDG	Glucose metabolism in tumors
	Choline transporter	^{11}C-choline	Tumor phospholipid synthesis
	thymidine uptake in DNA/RNA synthesis	^{18}F-FLT, ^{18}F-FMAU; ^{18}F-FU	Tumor cell proliferation
	$\alpha_V\beta_3$ integrin	^{18}F-galacto-RGD	Tumor angiogenesis
	HSV1-tk	^{18}F-FHBG	Suicidal gene therapy
	Hypoxia	^{18}F-FMISO; ^{64}Cu-, ^{60}Cu-ATSM	Tumor hypoxia
	Somatostatin receptor	^{64}Cu-TETA-octreotide	Neuroendocrine tumors
	Estrogen receptor	^{18}F-FES	Breast Cancer
	Androgen receptor	^{18}F-FDHT	Prostate Cancer
Cardiovascular Imaging	Cell metabolism	^{11}C Acetate	Cardiac metabolism
	Fatty acid metabolism	^{11}C Palmitate	Ischemia
	Adrenergic neurotransmission	^{11}C Metahydroxy-ephedrine	Heart failure
	Cardiac Sympathetic Neurons	^{18}F Norephinephrine	Cardiac sympathetic innervation
Neurological Imaging	Dopamine post synaptic receptors	^{11}C Raclopride	Schizophrenia, Addiction
	β-amyloid	^{11}C-PIB	Alzheimer's disease
	NK-1 Receptor	^{18}F SPARQ; ^{11}C-R116301	Depression, Anxiety
	Dopamine transporter	^{18}F FECNT	Schizophrenia, Addiction
	Dopamine metabolism	^{18}F DOPA	Schizophrenia, Addiction

Abbreviations: DG: 2-deoxyglucose; FDG: fluoro-2-deoxy-D-glucose; FLT: fluoro-L-thymidine; FMAU: 1-(2′-deoxy-2′-fluoro-β-D-arabinofuranosyl)thymine; FU: fluorouracil; galacto: galactose; RGD is a peptide sequence of arginine-glycine-aspartic acid; HSV1-tk: herpes simplex virus 1 – thymidine kinase; FHBG: fluoro-3-[hydroxymethyl]butyl)guanine; FMISO: fluoromisonidazole; ATSM: N^4-methylthiosemicarbazone; TETA: 1,4,8,11-tetraazacyclotetradecane-1,4,8,11-tetraacetic acid; FES: Fluoro-17-β-Estradiol; FDHT: Fluoro-5α-Dihydrotestosterone; PIB: 2-(4′-(methylamino)phenyl)-6-hydroxybenzothiazole (Pittsburgh Compound-B); NK-1: neurokinin-1; SPARQ: 2-fluoromethoxy-5-(5-trifluoromethyl-tetrazol-1-yl)-benzyl]([2S,3S]2-phenylpiperidin-3-yl)-amine); R116301: neurokinin-1 receptor antagonist hydroxybutanedioate; ^{18}F FECNT: 2β-carbomethoxy-3β-(4-chlorophenyl)-8-(2-[(18)F]-fluoroethyl)-nortropane; DOPA: dopamine.

Table 3

Commonly used SPECT tracers for clinical molecular imaging of diseases. Note, many agents image blood vessels and perfusion and/or excretion (labelled N/A for Molecular Target). Adapted from references:[105, 123]

Medical Imaging	Molecular Target/Localization	Radiotracer(s)	Clinical Applications
Oncological Imaging	Carcinoembryonic antigen	^{111}In altumomab pentetate	Colon Cancer
	Prostate-specific membrane antigen (PSMA)	^{111}In capromab pendetide/ProstaScint®	Prostate cancer
	Somatostatin receptor	^{111}In pentetreotide/Octreoscan®	Neuroendocrine cancers, gastroenteropancreatic tumors
	Tumor-associated glycoprotein	^{111}In satumomab pendetide/OncoScint®	Colorectal or Ovarian cancer metastasis
	Carcinoembryonic antigen	^{99m}Tc Arcitumomab/CEA-Scan®	Colorectal cancer
	Somatostatin receptor	^{99m}Tc Depreotide/Neotect®	Pulmonary and lung cancer
	CD20	^{90}Y Ibitumomab tiuxetan/Zevalin®	Non-Hodgkins lymphoma
	CD20	^{131}I Tositumomab/Bexxar®	Non-Hodgkins lymphoma
	NK-1 Receptor	^{90}Y-labelled substance P	Glioma
	Albumin	^{90}Y-MAA	Liver cancer
	N/A – (localizes in adrenergic tissue)	^{123}I-/^{131}I-MIBG	Neuroendocrine tumors
	N/A - Perfusion	^{99m}Tc-sulfur colloid	Sentinel lymph node metastasis/biopsy
	N/A - Perfusion	^{99m}Tc Sestamibi/Cardiolite®, Miraluma®	Breast cancer, lymph node metastasis
Cardiovascular Imaging	N/A - Perfusion	^{99m}Tc Teboroxime/Cardiotec®	Myocardial Perfusion
	N/A - Perfusion	^{99m}Tc Tetrofosmin/Myoview®	Myocardial Perfusion
	N/A - Perfusion	^{99m}Tc Sestamibi/Cardiolite®, Miraluma®	Myocardial Perfusion
Neurological Imaging	N/A - Perfusion	^{99m}Tc Bicisate (ECD)/Neurolite®	Cerebral Perfusion
	N/A - Perfusion	^{99m}Tc Exametazine (HMPAO)/Ceretec®	Cerebral Perfusion
	N/A - Perfusion	^{111}In pentetate/^{111}In DTPA®	CSF Kinetics
	Amphetamine receptor	^{123}I-iodoamphetamine	Neurodegenerative disorders; regional cerebral blood flow
	Phosphatidylserine	^{99m}Tc-HYNIC-annexin V	Dementia[124]
Gastrointestinal and Genitourinary Imaging	N/A – Perfusion/clearance	^{99m}Tc Disofenin (DISIDA)/Hepatolite®	Hepatobiliary
	N/A – Perfusion/clearance	^{99m}Tc Lidofenin (HIDA)/Technescan® HIDA	Hepatobiliary
	N/A – Perfusion/clearance	^{99m}Tc Gluceptate/Glucoscan®	Renal
	N/A – Perfusion/clearance	^{99m}Tc Mertiatide/Technescan® MAG3	Renal
	N/A – Perfusion/clearance	^{99m}Tc Pentetate (DTPA)/Techneplex®, Technescan®	Renal
	N/A – Perfusion/clearance	^{99m}Tc Succimer (DMSA)/DMSA	Renal, brain
	N/A – Perfusion/clearance	^{99m}Tc labelled red blood cells	Gastrointestinal bleeding and associated disorders; splenosis

Medical Imaging	Molecular Target/Localization	Radiotracer(s)	Clinical Applications
	N/A – Perfusion/clearance	^{99m}Tc-sulfur colloid	Splenosis
	Adrenal gland	^{131}I-6-β-iodomethyl-19-norcholesterol or ^{131}I-norcholesterol	Adrenocortical disorders
Musculoskeletal Imaging	Bone	^{153}Sm EDTMP/Quadramet®, or ^{99m}Tc-MDP	Palliative treatment of bone pain and bone metastases
	Hydroxyapatite crystals	^{99m}Tc Oxidronate (HDP)/Osteoscan® HDP	Bone

Abbreviations: CEA: carcinoembryonic antigen; CD20: leukocyte surface antigen; NK-1: neurokinin-1 receptor; MAA: macroaggregated albumin; MIBG: metaiodobenzylguanidine; ECD: ethyl cysteinate dimer; HMPAO: hexamethylpropyleneamine oxime; DTPA: diethylenetriamine-pentaacetic-acid; HYNIC: hydrazinonicotinamide; DISIDA: Di-isopropyliminodiacetic Acid; HIDA: *N*-(2,6 diethylphenylcarbomoylmethyl) iminodiacetic acid; Mag-3: mercaptoacetyltriglycine; DMSA: dimercaptosuccinic acid; EDTMP: ethylene diamine tetramethylene phosphonate; MDP: methylene diphosphonate; HDP: hydroxymethylene diphosphate. AGA: antigranulocyte antibody.

Table 4

Clinical applications with molecular MRI/MRS and Optical/Raman *in vivo* imaging.

Imaging Modality	Molecular Target	Contrast Agent	Example Clinical Application
MRS[8, 125–127]	Metabolites (e.g., lactate, choline, lipids, etc.)	N/A – spectroscopic measurement	Neurological diseases and abnormalities, metabolic disorders, and various cancers
Optical Tomography	Porphyrin	hexaminolevulinate (Hexvix); aminolevulinic acid	Bladder, laryngeal cancer[15]
Optical Tomography	Proteases	capthesin B- or MMP2/9-activated "smart" fluorescent probes	Atherosclerosis[24]
Optical Multiphoton Tomography	NAD(P)H, collagen	N/A – endogenous fluorescence	Skin cancer/diseases[13]
Raman Spectroscopy	N/A – Tissue specific spectra	N/A – Tissue specific spectra	Atherosclerosis;[21] colon cancer;[20, 128] breast cancer;[22] skin cancer;[113]

Abbreviations: MMP: matrix metalloprotease; NAD(P)H: nicotinamide adenine dinucleotide phosphate.

NIH-PA Author Manuscript

NIH-PA Author Manuscript

NIH-PA Author Manuscript

Table 5

Molecular targets, imaging probes, and drugs identified preclinically for imaging cancer with various modalities.

Molecular Target/Event	PET	SPECT	MRI/MRS	US	Hybrid Acoustic	Optical
			Imaging Modalities			
Apoptosis and/or Cytotoxicity Review:[129]	^{18}F-Paclitaxel (microtubule formation);[130][124] I-Annexin V; ^{18}F-Annexin V	^{99m}Tc-Annexin V	MRI: Annexin V-QDs with paramagnetic-lipid coating;[131] MRS: CH_2/CH_3 ratio			Annexin V-Cy5.5; Cy5.5-Caspase activity; Raman: SERS NPs conjugated to anti-BAX Ab or anti-BAD Ab[132]
Epidermal growth factor receptor (EGFR) Review:[133, 134]	^{11}C-Gefitinib; ^{11}C-Erlotinib/Tarceva; ^{64}Cu-Cetuximab	^{125}I-Anti-EGFR-Fab[135]	Anti-EGFR antibody-IO NPs		anti-EGFR Ab-gold nanorods[136]	Cy5.5-Cetuximab; Raman: anti-EGFR Ab-gold NPs[137]
Epidermal growth factor receptor type II (HER2/neu) Review:[134, 138]	[90]Y, [86]Y, or ^{68}Ga-Trastuzamab	^{111}In-Trastuzamab; [111]In-, [131]I-, or ^{99m}Tc-labeled anti-HER2 antibodies/fragments	Trastuzamab-MnO NP; Avidin-Gd^{3+}-anti-HER2 antibody; Herceptin-IO NPs		anti-HER2 Ab-gold nanorods;[136] Alexa fluor 750-herceptin[139]	Cy5.5-Trastuzamab; Cy5.5-anti-HER2 Ab; Raman: anti-HER2 Ab-SERS NPs[140]
Estrogen receptor Review:[134]	^{18}F-Tamoxifen; [94m]Tc-cyclofenil; ^{18}F-estradiol(FES)	^{131}I-Tamoxifen; tridentate [99m]Tc(I)-estradiol-pyridin-2-yl hydrazine				
Folate receptor Review:[134]	[66]Ga, ^{68}Ga-deferoxamine-folate; ^{18}F-folic acid	^{111}In-DTPA-folate; ^{99m}Tc-folate	PEG-G3-(Gd-DTPA)11-(folate)5		SWNT-folic acid[141]	Pyropheophorbide-peptide-folate
Hypoxia Reviews:[142-144]	[124]I-anti-cG250 (CAIX Ab); ^{18}F-FMISO, [124]I-FIAU; ^{18}F-FAZA, Cu-ATSM		MRI: ^{19}F oximetry, ^{19}F-FMISO; MRS: lactate measurement		oxyhemoglobin:de-oxyhemoglobin[145]	HIF-1α-reporter with GFP; Raman: lactate sensing[146]
Integrins (Tumor angiogenesis) Reviews:[147, 148]	^{64}Cu-RGD (SWNT); ^{64}Cu-RGD (QD); ^{64}Cu-RGD (SPIO); ^{64}Cu-knottin peptides[149]	^{111}In-perfluorocarbon NP-RGD	RGD peptide-Gd containing paramagnetic and fluorescent liposomes; RGD peptide-SPIOs	Knottin-RGD conjugated MBs;[65] RGD MBs; Anti-β3 Ab-MB; Echistatin-coated MBs; β3-targeted perfluoro-carbon NP	SWNT-RGD;[45] αvβ3 peptide-ICG[50]	RGD-QD705; RGD-Rhodamine/PE-liposomes; Cy5.5-knottin peptides; Raman: SWNT-RGD[41]
Metabolism/Proliferation	^{18}F-FDG; ^{18}F-FLT; ^{18}F-FBC[151]					Cy5.5-2DG[152]
Proteases Review:[153]	Radiolabeled small molecule MMP inhibitors[154]	Radiolabeled small molecule MMP inhibitors[154]	MMP2-specific peptide-Gd^{3+}-DOTA "smart probe"[155]			Cyanine-peptide to capsesin; Cy5.5-peptide to MMP
Prostate Specific Membrane Antigen (PSMA)	^{64}Cu-anti PSMA Ab[156]	^{123}I-labelled glutamate-urea-lysine analogues;[157][99m]Tc-chelates[158]	MRI: anti-PSMA Ab-IO NPs[159]			YC-27(3) fluorescent probe;[160] QD-anti PSMA Ab[161]
Reporter gene expression[162, 163]	HSV1-tk: ^{18}F-FHBG, ^{18}F-FHPG, ^{18}F-FMAU, ^{18}F-FEAU	HSV1-tk: ^{123}I-FIAU	βgal (EgadMe); Transferrin receptor (Transferrin-MION); Ferritin (iron); lysine rich protein		βgal[164]	luciferases (bioluminescence); fluorescent proteins (Fluorescence)

	Imaging Modalities					
Molecular Target/Event	PET	SPECT	MRI/MRS	US	Hybrid Acoustic	Optical
Vascular endothelial growth factor (VEGF) receptor (VEGFR) (Tumor angiogenesis) Reviews:[147,148]	[89]Zr-Avastin; ^{64}Cu-DOTA-VEGF; ^{64}Cu-DOTA-VEGF (peptide)	^{111}In-Avastin; ^{125}I-VEGF[165], (^{125}I or ^{99}Tc)-VEGF[121], ^{111}In-hnTf-VEGF		Anti-VEGFR2 Ab-MB;[59] KDR peptide-conjugated MBs[30]		VEGF-Cy5.5; VEGF-QD

Abbreviations: QDs: quantum dots; SERS: surface-enhanced Raman scattering; NPs: nanoparticles; Ab: Antibody; BAX: protein involved in mitochodrial stress-associated apoptosis; BAD: a BCL-2 family member protein that promotes apoptosis; Fab: fragment antibody; IO: iron oxide; DTPA: diethylenetriamine-pentaacetic-acid; PEG: polyethylene glycol; Gd/Gd^{3+}: Gadolinium; MnO: Manganese oxide; FES: fluoroestradiol; SWNT: single-walled nanotubes; CAIX: carbonic anhydrase IX; FMISO: fluoromisonidazole; FAZA: 1-α-D-(2-deoxy-2-fluoroarabinofuranosyl)-2-nitroimidazole; ATSM: N^4-methylthiosemicarbazone; HIF-1α: hypoxia inducible factor type 1α; GFP: green fluorescent protein; RGD: is a peptide sequence of arginine-glycine-aspartic acid; SPIO: superparamagnetic iron oxide; MBs: microbubbles; ICG: iodocyanine green; PE: phycoerythrin; FDG: fluoro-2-deoxy-D-glucose; FLT: fluoro-L-thymidine; FEC: fluoroethylcholine; 2DG: 2-deoxyglucose; MMP: matrix metalloprotease; DOTA: 1,4,7,10-tetraazacyclododecane-1,4,7,10-tetraacetic acid; YC-27(3): specific name for a small molecule NIRF-imaging agent synthesized from a N-hydroxysuccinimide portion of PSMA-binding urea and a NIR dye (IRDye 800);160 HSV1-tk: herpes simplex virus 1 thymidine kinase; FHBG: 9-[(3-fluoro-1-hydroxy-2-propoxy) methyl] guanine; FHPG: 9-[(3-fluoro-1-hydroxy-2-propoxy) methyl] guanine; FIAU: 9-[(3-fluoro-1-hydroxy-2-propoxy) methyl] guanine; βgal: β galactosidase; EgadMe: (1-(2-(b-galactopyranosyloxy)propyl)-4,7,10-tris(carboxymethy)-1,4,7,10-tetraazacyclododecane)gadolinium(III); MION: monocrystalline iron oxide; hnTf: n-lobe of human transferrin; VEGFR2: VEGFR type 2; KDR: kinase insert domain receptor (human VEGFR2).